Quinoline-Pyrimidine Hybrids: Synthesis, Antiplasmodial Activity, SAR, and Mode of Action Studies

ARTICLE *in* JOURNAL OF MEDICINAL CHEMISTRY · DECEMBER 2013

Impact Factor: 5.45 · DOI: 10.1021/jm4014778 · Source: PubMed

Kamaljit Singh
Guru Nanak Dev University

Peter Smith
University of Cape Town

Carmen Abriette de Kock
University of Cape Town

Journal of Medicinal Chemistry

Article

pubs.acs.org/jmc

Quinoline−Pyrimidine Hybrids: Synthesis, Antiplasmodial Activity, SAR, and Mode of Action Studies

Kamaljit Singh,*,† Hardeep Kaur,† Peter Smith,‡ Carmen de Kock,‡ Kelly Chibale,§ and Jan Balzarini∥

†Department of Chemistry, UGC Centre of Advance Study-I, Guru Nanak Dev University, Amritsar, Punjab 143005, India

‡Division of Pharmacology, Department of Medicine, University of Cape Town, Observatory 7925, South Africa

§Department of Chemistry, Institute of Infectious Disease and Molecular Medicine, University of Cape Town, Rondebosch 701, South Africa

∥Rega Institute for Medical Research, KU Leuven, Minderbroedersstraat 10, B-3000 Leuven, Belgium

Supporting Information

ABSTRACT: For the treatment of malaria which affects nearly 200 million people each year and the continued exacerbation by the emergence of drug resistance to most of the available antimalarials, the "covalent bitherapy" suggests hybrid molecules to be the next-generation antimalarial drugs. In this investigation, new hybrids of 4-aminoquinoline and pyrimidine moieties that show antiplasmodial activity in the nM range against chloroquine-resistant as well as chloroquine-sensitive strains of *Plasmodium falciparum* have been prepared. Cytotoxicity evaluation and mode of action of most potent hybrid molecule have been conducted.

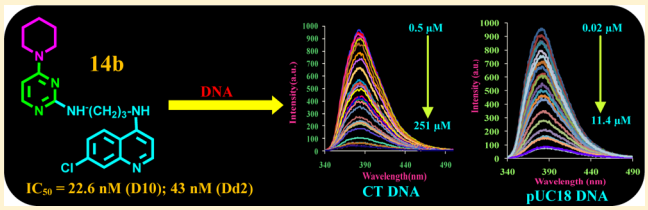

INTRODUCTION

Malaria is one of the major infectious diseases[1,2] along with tuberculosis and HIV/AIDS which infects over 200 million people each year and results in over 1 million deaths. Malaria is endemic in more than 100 countries throughout the tropics and in some temperate regions. According to the latest WHO estimates, malaria accounted for 219 million illnesses and an estimated 660000 deaths worldwide in 2010; about 90% of all malaria deaths occur in Africa and were due to *Plasmodium falciparum* infections of young children.[3,4] The traditional drugs such as chloroquine (**1**, CQ), pamaquine **2**, and mefloquine **3** (Figure 1), which were once significantly active and affordable, lost significance owing to the emergence of parasite strains that are resistant to such drugs. The drug resistance of CQ is strongly linked to mutations in the gene that give rise to the protein, PfCRT (*P. falciparum* chloroquine resistance transporter), located in the parasite's digestive vacuole (DV) membrane.[5−7] Consequently, excessive export of CQ from its site of action and decrease in the accumulation of the drug in the DV eventually results in loss of antimalarial activity.[8,9] Small molecules structurally related to the 4-aminoquinoline motif are known to exert antimalarial action through prevention of polymerization of toxic heme, leading to its accumulation which results in parasite death.[10] Heme targeting, molecules that act on several other targets such as phospholipids, tyrosine kinase,[11] DNA via intercalation,[12] hemoglobin degrading proteases,[13,14] and phospholipases,[13−15] have shown a useful level of antimalarial action.

To tackle the development of resistance to the antimalarial drugs, the concept of hybrid drugs (covalent bitherapy) has triggered a new strategy in drug design which involves linking two drugs with intrinsic activity into a single agent.[16,17] In most such hybrids, two pharmacophores have independent modes of action against different targets that make the emergence of drug resistance less likely. Recently, the fast-acting artemisinin has been combined with the slow-acting quinine into a hybrid drug **4** for malaria.[18] Drugs based on fully synthetic peroxidic molecules, trioxaquines represented by **5** (DU1301)[19] and **6** (PA1103/SAR116242), constitute other examples of the synthetic hybrid molecules containing a 1,2,4-trioxane motif linked to a 4-aminoquinoline unit and have shown promising activity against early erythrocytic stages of *P. falciparum* as tested against both CQ-resistant (CQ^R) and CQ-sensitive (CQ^S) strains.[20,21] In addition to alkylation of heme by trioxaquine, the aminoquinoline partner of **5** and **6** promotes heme stacking and prevents polymerization of heme into the nontoxic hemazoin and thus act at different stages of the parasite's life cycle through a dual mode of action.

The hybrid antimalarials featuring quinoline as one partner are represented (**A**−**L**, Figure 2) by quinoline−cinnamic acid **A**,[22] quinoline−ferrocenophane **B**,[23] quinoline−rhodanine **C**,[24] quinoline−primaquine **D**,[25] quinoline−triazine **E**,[26] quinoline−isatin **F**,[27] quinoline−clotrimazole **G**,[28] quinoline-γ-hydroxy-γ-lactam **H**,[29] quinoline−furoxan **I**,[30] quinoline−hydroxypyridone **J**,[31] quinoline−pyrimidines **K**,[32−34] and quinoline−pyrimidine carboxylates **L**,[35,36] etc., that possess promising activities against CQ^R strains and hit different targets. Spurred

Received: September 21, 2013
Published: December 19, 2013

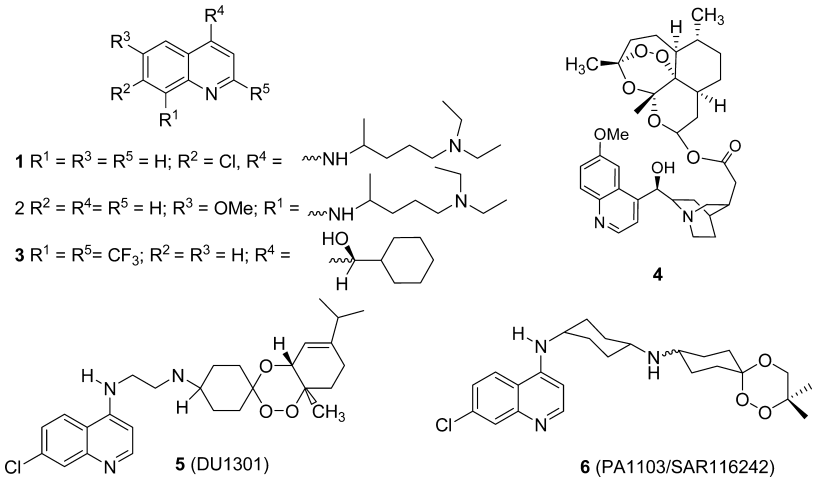

Figure 1. Quinoline antimalarials.

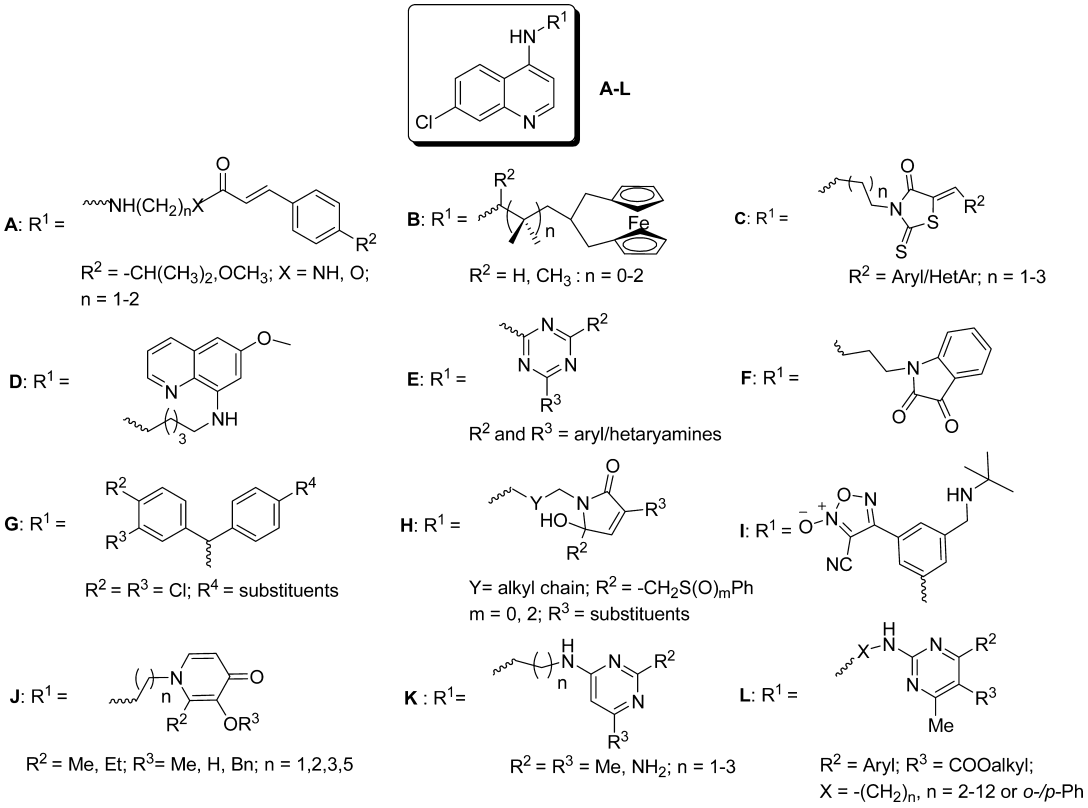

Figure 2. Representative quinoline hybrid antimalarial compounds **A**−**L**.

by the therapeutic advantage of the hybrid antimalarials, recently we reported on the structure−activity relationship, cytotoxicity, and mode of action studies of some quinoline−pyrimidine carboxylate hybrids **L** (Figure 2).[35,36] It was found that the activity of these hybrids was dependent upon the length of the linker (aromatic/aliphatic) connecting the two pharmacophores as well as the substituents on the pyrimidine motif. However, these hybrids displayed quite a high toxicity and ClogP values.[35,36] In this investigation, we report the synthesis, evaluation of in vitro antiplasmodial activity, physicochemical properties such as acid dissociation constant (pK_a), aqueous solubility and distribution coefficient (log D), and mechanism of action studies on new hybrids comprising of 4-aminoquinoline unit linked to pyrimidine motifs derived from uracil, lacking a carboxylate at the 5-position. Moreover, side chain diversity was also explored by varying the nature and length of the linker between the two "N" atoms as well as the substitution pattern and basicity of the distal amino group. Furthermore, binding experiments (^{1}H NMR, FTIR, and LCMS) were performed with the heme (monomeric and μ-oxo) as well as DNA (CT-DNA and pUC18 DNA) to explore possible mode of antimalarial action of these hybrids.

■ CHEMISTRY

The quinoline−pyrimidine hybrids were synthesized in an economical way using an expedient approach that entails linking the 2,4-dichloropyrimidine **8** unit with appropriate derivatives of 4-amino-7-chloroquinoline **9** or morpholine **10** as

Scheme 1. Synthesis of 4-Aminoquinoline−Pyrimidine Hybrids

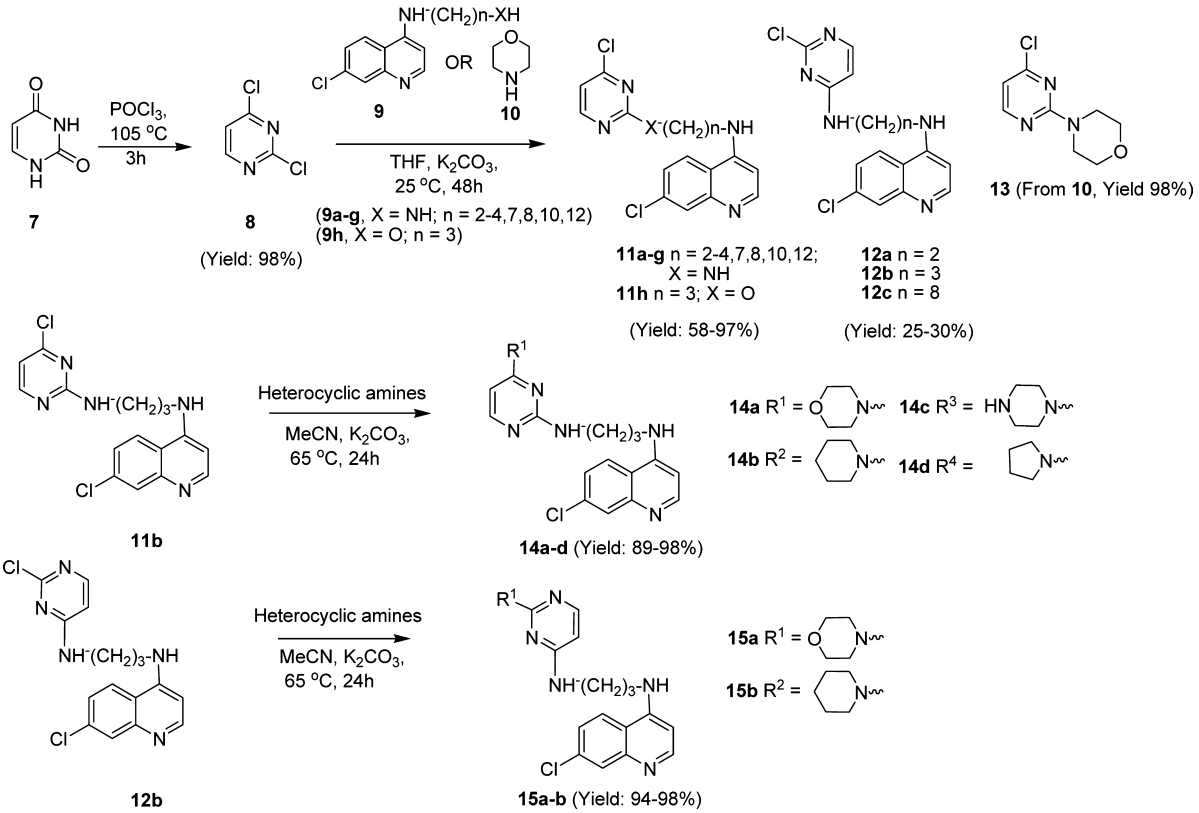

outlined in Scheme 1. The reaction of uracil **7** with refluxing $POCl_3$ under solvent-free conditions readily furnished **8** in 98% yield. Treatment of 4,7-dichloroquinoline with an excess amount of appropriate diaminoalkane or aminoalcohol under inert atmosphere conditions furnished corresponding *N*-(7-chloro-4-quinolyl)diaminoalkane **9** in quantitative yield, as described.[37] The nucleophilic substitution reaction of **8** with appropriate **9** or morpholine **10** in the presence of a base in THF afforded 4-chloro-substituted hybrids **11a−h** in 58−97% yield and 2-chloro-substituted structural isomers **12a−c** in 25−30% yields (Table 1), after column chromatographic separation. Finally, substitution of a second chloro substituent of **11b** or **12b** with different heterocyclic amines in acetonitrile gave another set of hybrids **14** (89−98%) and **15** (94−98%), respectively (Table 1). The structures of all the compounds were established on the basis of spectral (^{1}H NMR, ^{13}C NMR, LCMS, FTIR) as well as microanalytical data (vide experimental). Further, heteronuclear multiple quantum correlation (HSQC) and heteronuclear multiple bond correlation (HMBC) NMR experiments were recorded for the isomeric **11b**/**12b** and **14a**/**15a** pairs (Supporting Information, Section S1) to corroborate the structures of these compounds. To unequivocally establish the structures of the isomeric compounds **14a**,**b** and **15a**,**b**, the structure of **14a** was additionally confirmed by determing the single crystal X-ray structure (Supporting Information, Table S1). The Ortep diagram is given in Figure 3. The structures of **15a** as well as the pair **14b**/**15b** were established by analogy with the spectroscopic data of **14a**.

RESULTS AND DISCUSSION

Antiplasmodial Activity and Structure−Activity Relationships (SARs). The in vitro antiplasmodial activity of the hybrids **11−15** was evaluated against the D10 (CQ^S) as well as Dd2 (CQ^R) strains of *P. falciparum* using CQ, artesunate (ASN), and MMV390048[38] as positive controls. Among the 18 compounds tested, five compounds displayed IC_{50} values in the range of 22−70 nM against D10 strain. One of the compounds bearing the 2-morphonylpyrimidine core (**13**) was devoid of significant activity, and the remaining compounds had IC_{50} values ranging between 113 and 4310 nM (Table 1) as described below.

Structure−activity relationship studies indicate that increasing the length of the methylene spacer from $-(CH_2)_2-$ to $-(CH_2)_{12}-$ in **11a−g** and **12a−c** has a significant effect on the antiplasmodial activity. Among the C-2 quinolinyl hybrids **11a−g**, the antiplasmodial activity against both CQ^S and CQ^R increases only up to a $-(CH_2)_4-$ spacer (**11a−c**, Table 1), further chain lengthening resulted in reduction of the activity against the CQ^S strain. These results are in accordance with the trend observed in case of *N*,*N*-bis-(7-chloroquinolin-4-yl)alkane diamines, wherein the alkyl spacer consisting of four carbon atoms showed optimum potency.[39] On the other hand, the antiplasmodial activity against the CQ^S strain of the C-4 quinolinyl-substituted hybrids **12a−c**, bearing $-(CH_2)_2-$, $-(CH_2)_3-$, and $-(CH_2)_8-$ alkane spacers, respectively, is maximized in **12b**, which has three methylene groups. Further, the C-2 and C-4 quinolinyl structural isomers **11b** and **12b**, respectively, bearing a three carbon spacer, displayed (Table 1) comparable (IC_{50} 244 nM, **11b**; IC_{50} 270 nM, **12b**) activities against CQ^S (D10) strain; although against the CQ^R (Dd2) strain, **12b** was nearly 2.3-fold more active. The above trend of

Table 1. In Vitro Antimalarial Activity of Compounds 11−15 against *P. falciparum* (CQ^S) D10 Strain and (CQ^R) Dd2 Strain for $n = 3$ (n = Number of Replicates)

S. no	Structure	Yield (%)	D10 IC_{50} (nM)[a,b]	Dd2 IC_{50} (nM)[b,c]	CLogP[d]	Minimum cytotoxic concentration (μM)[e,f]	CC_{50} (μM)[g,h]	SI[i]
1, CQ			21.8±3.4	140±0.18	5.1	30±1[j]	-	-
ASN			6.3±0.71	31.2±8.0	1.06	-	-	-
MMV 390048			9.01±3.78	17.8±0.19	2.22	-	-	-
11a	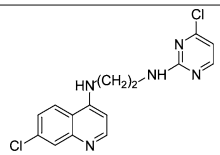	58	2510±374	7678±373	4.41	>100	>100	12.53
11b	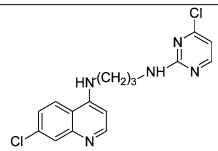	65	244±4.4	478±54.6	4.81	>100	>100	>209
11c	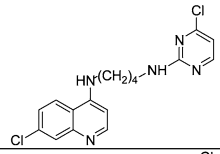	56	179±18.8	193±11.2	4.93	100	>100	>518
11d	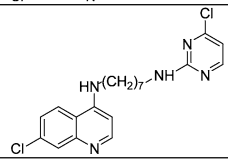	64	383±33.4	nd	6.52	4	>100	-
11e	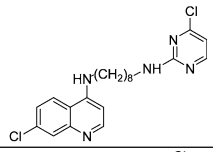	65	1057±40.9	nd	7.05	20	10	-
11f	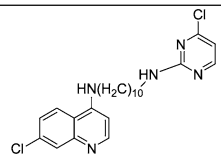	60	3340±126	nd	8.10	4	4.4	-
11g	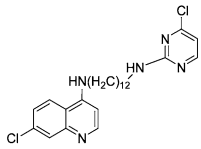	58	4310±326	nd	8.19	20	19	-
11h	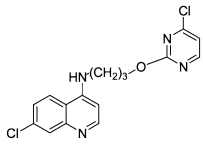	97	304±33.9	204±16.7	4.83	>100	>100	>490
12a	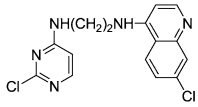	25	1430±179	nd	4.41	4	>100	-

Table 1. continued

S. no	Structure	Yield (%)	D10 IC_{50} (nM)[a,b]	Dd2 IC_{50} (nM)[b,c]	CLogP[d]	Minimum cytotoxic concentration (μM)[e,f]	CC_{50} (μM)[g,h]	SI[h]
12b	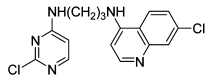	25	270±5.1	207±9.1	4.81	>100	>100	>483
12c	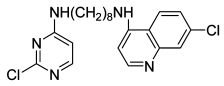	30	912±103	883±108	7.05	4	8.0	9
13	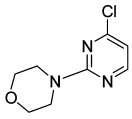	98	14980±1280	nd	0.99	>100	>100	-
14a	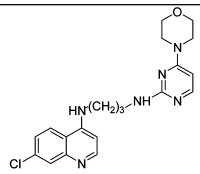	97	55±1.7	158±7.4	4.61	>100	>100	>632
14b	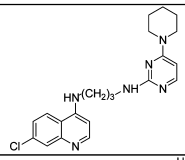	98	22.6±2.2	43±5.3	6.15	100	9.8	228
14c	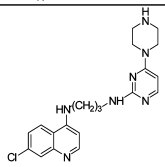	97	113±14.4	2003±240	3.73	100	74	36
14d	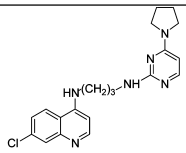	89	28.7±2.1	151±14.5	5.56	100	49	327
15a	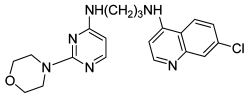	98	70±8.9	404±155	4.61	100	>100	>247
15b	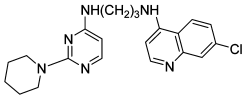	94	65.5±1.6	166±19.5	6.15	20	55	334

[a]CQ sensitive strain. [b]Data represents the mean of three independent experiments. [c]CQ resistant strain. [d]Calculated from Chem Draw Ultra 11.0 plus. [e]Required to cause a microscopically detectable alteration of the normal cell morphology. [f]Determined on HeLA cell cultures (reference drugs used: DS-5000 (μg/mL)/MIC >100, and (S)-DHPA/MIC (μM) >250). [g]Determined on Crandell–Rees feline kidney cells (CRFK) cells. [h]50% cytotoxic concentration, as determined by measuring the cell viability with the colorimetric formazan-based MTS assay (reference drugs used: HHA CC_{50}/MIC >100, UDA CC_{50}/MIC 63.2 and, Ganciclovir CC_{50}/MIC >100) [i]Selectivity Index (SI) is calculated as CC_{50}/IC_{50} (Dd2 strain) ratio. [j]IC_{50} (50% inhibitory concentration for cell proliferation). nd = not determined.

activity for the structural isomers was not observed when the chloro substituent of **11b** and **12b** was replaced by either morpholine or piperidine to create **14a,b** and **15a,b**, respectively. Thus, while **14a** bearing a morpholino group at the C-4 position of the pyrimidine was more effective against the D10 strain, **14b** bearing a piperidine group at the same position was active against both Dd2 (IC_{50} 43 nM) as well as D10 (IC_{50} 22.6 nM) strains. Both **15a** and **15b** showed almost similar activity (IC_{50} 70 nM, **15a**; IC_{50} 65.5 nM, **15b**) against D10 strain. Replacing the more basic diaminoalkyl linker of **11b** with a relatively less basic alkoxy amino linker in **11h** resulted in a decrease in the antiplasmodial activity of **11h**, which may be attributed to the reduced accumulation of **11h** in the DV of the parasite in analogy to the work reported in the literature[40] and supporting the notion that the basicity of an alkyl chain linker plays a crucial role in determining the activity of quinoline-based antimalarials.[37]

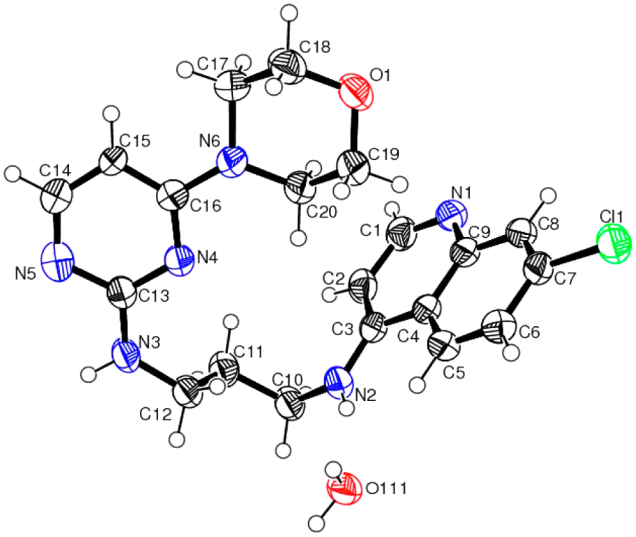

Figure 3. X-ray structure and crystallographic numbering of **14a** (CCDC number 974702).

The pK_a of the titratable nitrogens were measured for the series of compounds **11−15**. The pK_a data (Table 2) shows that compounds **11a−11g** in which the chain length of the linker increases from 2 to 12 carbon atoms, the first three members **11a−11c** recorded an increasing trend in basicity, while increasing the chain length beyond four carbons up to 10 carbons (**11d−11g**) recorded a decreasing trend in the experimentally determined pK_a values. The more interesting comparison was evident in the members **11b** and **11h**, in which the more basic aminoalkyl linker of **11b** was replaced with less basic alkoxy amino linker (**11h**), the pK_a corresponding to the quinoline group decreased from 8.21 to 8.12 and the pK_{a1} 7.10, corresponding to the linker NH in **11b**, was absent for **11h**. This supports the observed trend in the antiplasmodial activity of **11b** and **11h** (Table 1). Among the compounds **12a−c**, the pK_a value of the less active **12a** (IC_{50} 1430 ± 179) with a two carbon chain was considerably lower than the more active **12b** (IC_{50} 270 ± 5.1), the three carbon counterpart. The pK_a value increased marginally when the chain length of the linker increased to eight carbon analogue **12c**. Hence, the length and nature of the spacer linking a quinoline and pyrimidine moieties appears to play a crucial role in determining the antiplasmodial activity of **11−15**.

Physicochemical parameters such as aqueous solubility (S_W) and lipophilicity are important determinants for drug absorption as well as pharmacokinetic profiles. A good balance of the lipophilic−hydrophilic properties has been reported to influence the way a drug molecule passes through biological membranes and barriers to eventually enter the systemic circulation. Thus, optimal solubility to both water and octanol is a prerequisite for drugs intended to be administered orally.[41−43]

The aqueous solubility and the distribution coefficient (log D), a pH dependent version of the partition coefficient (log P) of all compounds, is compiled in Table 2. The solubility in octanol (S_{OC}) was calculated from the experimental S_W and log D data using the equation: log S_{OC} = log D + log S_W. The aqueous solubility (S_W) in PBS buffer and log D in an n-octanol/buffer mixture at the cytosolic pH 7.4 of the parasite[44] was determined using HPLC (Supporting Information, Section S1).[45] The data in Table 2 shows that all the compounds exhibit appreciable S_W in μM range, which decreases as the length of spacer increases from 2 to 12 carbon atoms. Further,

Table 2. Acid Dissociation Constants (pK_a), Aqueous Solubility (S_w), Distribution Coefficients (log D), and Solubility in Octanol (S_{OC}) of Compounds 11−15

compd	pK_a[a]		M_w (g/mol)	S_W (μM)[e]	log D[e]	S_{OC} (μM)[f]
	pK_{a1}[b]	pK_{a2}[b]				
11a	7.01	8.10	334.2	0.90 ± 0.07	0.501 ± 0.021	2.85
11b	7.10	8.21	348.2	0.40 ± 0.05	0.657 ± 0.081	1.81
11c	7.45	8.64	362.2	0.70 ± 0.09	0.742 ± 0.016	3.86
11d	6.82	8.11	404.3	0.13 ± 0.04	1.162 ± 0.017	1.92
11e	6.74	8.00	418.3	0.09 ± 0.03	1.510 ± 0.143	2.91
11f	5.97	7.85	446.4	0.07 ± 0.01	1.989 ± 0.261	6.82
11g	nd	nd	474.4	0.05 ± 0.01	2.590 ± 0.109	19.40
11h	na	8.12	349.2	0.20 ± 0.06	1.040 ± 0.270	2.19
12a	5.85	8.20	334.2	0.68 ± 0.08	0.489 ± 0.034	2.09
12b	7.22	8.62	348.2	0.60 ± 0.02	0.229 ± 0.059	1.01
12c	7.29	8.43	418.3	0.08 ± 0.01	1.480 ± 0.181	2.41
13	na	na	199.6	9.00 ± 0.36	0.130 ± 0.026	12.14
14a	5.20	7.95	398.1	0.53 ± 0.12	0.257 ± 0.068	0.95
14b	7.18	8.33	396.9	0.25 ± 0.09	0.845 ± 0.111	1.74
14c[c]	5.53	9.17	397.9	0.60 ± 0.06	0.102 ± 0.018	0.75
14d	6.80	8.08	382.9	0.22 ± 0.09	0.756 ± 0.094	1.25
15a	7.30	8.70	398.1	0.55 ± 0.12	0.363 ± 0.083	1.27
15b	7.35	8.63	396.9	0.32 ± 0.07	0.801 ± 0.053	2.02
1, CQ	8.30[d]	10.98	319.8	nd	nd	nd

[a]The pK_a data represents mean of the three determinations obtained at 298.1 K. [b]pK_{a1} represent the pK_a of the secondary nitrogen atom bonded to the pyrimidine core and pK_{a2} represents the pK_a of the quinoline N. [c]pK_{a3} corresponding to the secondary NH of piperazine, bonded to pyrimidine core is found to be 6.85. [d]pK_{a1} represent the pK_a of the side chain tertiary nitrogen. [e]Experimental data represent the mean ± SD of three independent measurements. [f]Solubility in octanol (S_{OC}) at pH 7.4 was calculated from experimental aqueous solubility (S_W) and distribution coefficient log D (n-octanol/PBS buffer) at pH 7.4 using log S_{OC} = log D + log S_w. nd = not determined. na = not applicable.

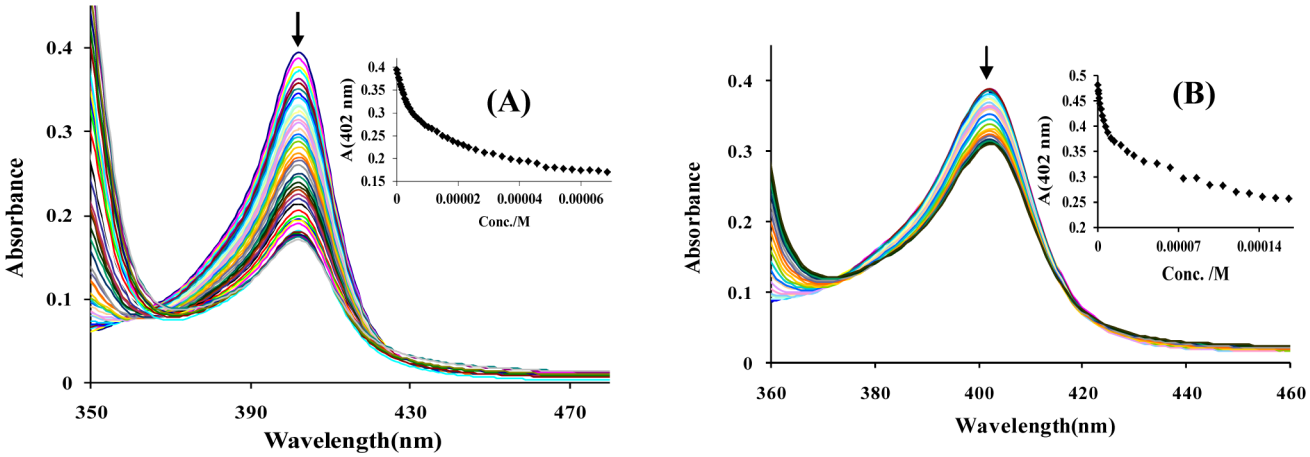

Figure 4. Titration of monomeric heme (2.4 μM) (A) at pH 7.4 (0.02 M HEPES buffer in aqueous DMSO solution) and (B) pH 5.6 (0.02 M MES buffer in aqueous DMSO solution) with increasing concentration of **14b** (0–69 μM in DMSO). (Inset: plot of A_{402} nm vs conc of **14b**).

compared to the compounds with long chain (7–12 carbon atoms) diamino linkers **11d–11g** and the aminoalkoxy linker in **11h**, the most active compound **14b** of the series depicted higher aqueous solubility (Table 2).

Further, we evaluated the trends in the antiplasmodial activity upon replacing the chloro substituent of the representative hybrids **11b** and **12b** with cyclic amines (morpholine, piperidine, piperazine, and pyrrolidine) of varying basicity to generate compounds **14a–d** and the structural isomers **15a–b**, respectively (Scheme 1 and Table 1). Overall, it was found that all compounds bearing cyclic amines **14a–d** and **15a–b** were more active than their precursor Cl-substituted analogues **11b** and **12b** against both D10 and Dd2 strains. In the series of the compounds **14a–d**, the antiplasmodial activity increased in the order **14b** > **14d** > **14a** > **14c** against D10 strain (Table 1), while **15a** displayed activity similar to **15b**. Unlike **11b** and **11h**, the observed trend of antiplasmodial activity in **14a–14d** does not follow the trend of their pK_a (Table 2) values but is consistent with the lipophilicity trend [ClogP: **14b** (6.15) > **14d** (5.56) > **14a** (4.61) > **14c** (3.73)] as shown in Table 1 as well as log *D* [**14b** (0.845) > **14d** (0.756) > **14a** (0.257) > **14c** (0.102)] values shown in Table 2. The more basic compound **14c** recorded an additional p*K*a (pK_{a3}, Table 2) value corresponding to the additional nitrogen of piperazine. Similarly, the antiplasmodial activities of **15a** and **15b** are also in the order of their ClogP [**15b** (6.15) > **15a** (4.61)] as well as log *D* [**15b** (0.801) > **15a**(0.363)] values (Table 2). Thus, the compound **14b** exhibited the highest antiplasmodial activity (IC_{50} 43 nM against Dd2 strain, respectively) within the series, which is 3.2-fold higher than the standard chloroquine against Dd2 strain. It is important to recall that in addition to basicity and lipophilicity, other factors such as binding with heme also contribute to the antiplasmodial activity. Thus, for the structural isomeric 4-aminoquinoline hybrids **14a**/**15a** and **14b**/**15b**, which exhibit identical ClogP values (Table 1), variation in antimalarial activity may in part be attributed to the way these compounds bind to heme or other drug targets. Further, the compound **13** lacking a 7-chloroquinolinyl group is devoid of any antiplasmodial activity further points to the involvement of the quinoline moiety for the observed antiplasmodial activity of hybrids **11**, **12**, **14**, and **15**.

Thus, these hybrids which have molecular weights below 500 (Table 2) exhibit antiplasmodial activities in the nanomolar range against both the CQ^S and CQ^R strains of *P. falciparum*. The most active compound of this series **14b** (43 nM) displayed activity greater than CQ against the Dd2 strain, which also approaches that of artesunate (31.2 nM). Further, the SAR study revealed that the alterations in length and nature of methylene spacer as well as incorporation of a variety of heterocyclic rings on the pyrimidine motif have considerable effect on antiplasmodial activity.

Cytotoxicity and Antiviral Activity. The cytotoxicity (CC_{50} values, Table 1) of all the synthesized hybrids **11–15** was determined against various (HeLa, Vero, CRFK, Hel, and MDCK) mammalian cell cultures (Supporting Information, Tables S2–S7). These studies reveal that most of the compounds are noncytotoxic at submicromolar concentrations against any of the tested cell cultures. Further, the ratio of the cytotoxicity (CC_{50} in μM) and in vitro antiplasmodial activity (IC_{50} in nM for Dd2 strain) enabled the determination of a selectivity index (SI) for these compounds. Nine compounds displayed a fairly good selectivity index (SI) ranging from 209 to 632 (Table 1), whereas two compounds, **12c** and **14c**, exhibited only moderate SI values (9 and 36). All the hybrids of the series displayed structure-dependent SI values which are greater than 209, except **12c** and **14c**.

CQ shows inhibitory effects against several viruses, including human immunodeficiency virus type 1 and hepatitis B virus. It is a weak base that increases the pH of acidic vesicles. When added extracellularly, the nonprotonated portion of CQ enters the cell,[46] where it gets protonated and concentrated in acidic, low-pH organelles such as endosomes, Golgi vesicles, and lysosomes.[47,48] CQ can affect virus infection in many ways, and the antiviral effect depends in part on the efficiency of endosome-mediated virus entry.[46–50] Thus, we determined in vitro antiviral activities of **11–15** against (i) herpes simplex virus-1 (HSV-1; KOS), herpes simplex virus-2 (HSV-2; G), vaccinia virus, vesicular stomatitis virus, herpes simplex virus-1 (KOS TK-ACV^R) in HEL cell cultures, (ii) parainfluenza-3 virus, reovirus-1, Sindbis virus, Coxsackie virus B4, Punta Toro virus in Vero cell cultures, (iii) influenza A virus (H1N1 and H3N2) and influenza B virus in MDCK cell cultures, (iv) vesicular stomatitis virus, Coxsackie virus B4, respiratory syncytial virus in HeLa cell cultures, (v) cytomegalovirus using AD-169 and Davis strain in HEL cell cultures, (vi) varicella-zoster virus (VZV) in HEL cell cultures, (Supporting Information, Tables S2–S7), and (vii) feline corona virus

Table 3. Binding Constant (log K) for 14b and CQ

compd	monomeric heme log $K \pm \sigma$		μ-oxo heme log $K \pm \sigma$	CT DNA log K	pUC18 DNA log K
	pH 5.6	pH 7.4	pH 5.8		
14b	4.5909 ± 0.0161	4.6344 ± 0.3050	5.8427 ± 0.1044	3.64	3.99
CQ	4.65 ± 0.052	5.15 ± 0.176	5.58 ± 0.006	nd	nd
stoichiometry	1:1		1:1		nd

(FIPV) and feline herpes virus activity in CRFK cell cultures (Supporting Information, Table S8). No significant antiviral activity was noted at subtoxic concentrations, pointing to some degree of selectivity of the antiplasmodial agents.

Mode of Action Studies. *Heme Binding Studies.* CQ and related 4-aminoquinoline antimalarials bind to FPIX via $\pi-\pi$ stacking interaction of the quinoline ring with the porphyrin ring, thus preventing the sequestration of toxic heme to hemozoin.[10] One of the possible mechanisms of antimalarial action of quinoline−pyrimidine hybrids is through inhibition of hemozoin formation. Therefore, we decided to evaluate the binding of the most potent compound **14b** of the series with heme. The stepwise addition of small increments of **14b** (0−69 μM, DMSO) into a constant concentration of monomeric heme (2.4 μM) in 0.02 M HEPES buffer in aqueous DMSO at pH 7.4 and at the plasmodial food vacuole acidic pH 5.6 (0.02 M MES buffer in aqueous DMSO) resulted in a substantial decrease in intensity of the Fe(III) PPIX Soret band at 402 nm with no shift in the absorption maximum (Figure 4). Solvent (DMSO) does not affect the binding of **14b** with heme at the pH values used in this experiment. A 1:1 stoichiometry of the most stable complex of **14b** with monomeric heme at pH 7.5 and 5.6 was established from the Job's plot (Supporting Information, Figure S1). The association constants (Table 3) were calculated by analyzing the titration curves obtained at pH 7.4 using HypSpec, a nonlinear least-squares fitting program.[51] The titration of CQ with heme were also performed under identical conditions, and the binding constants were calculated for comparison purposes. Table 3 shows that the association constants for the complexes formed between monomeric heme and **14b** (log K 4.63) is less than those of the standard antimalarial drug CQ (log K 5.15). Furthermore, the decrease of apparent pH from 7.4 to 5.6 (Table 3) has little effect on the binding constants, indicating that binding is stronger even at acidic pH.

The binding of **14b** with monomeric heme was further supported by the ^{1}H NMR titration. The titration experiment was performed by recording the ^{1}H NMR spectra of **14b** in 40% DMSO:D_2O/D_2SO_4 (10 μL) after addition of heme (10 and 30 mol %) dissolved in DMSO. Shift in both the aromatic as well as aliphatic proton signals of **14b** (Figure 5) was noted upon addition of 10 mol % of heme to the solution, indicating binding of **14b** with heme. However, further addition of heme led to broadening of the peaks which may be due to the paramagnetic effect of Fe(III) of the ferriprotoporphyrin(IX).

Further, the mass spectral analysis of an equimolar (5 μmol) solution of hemin chloride and **14b** depicted an intense molecular ion peak at 1012.2993 Da (Figure 6A), corresponding to the molecular formula $C_{55}H_{57}ClFeN_{10}O_4$ and further corroborating the formation of 1:1 complex. Thus, on the basis of this data as well as the literature precedence,[52] we propose that **14b** interacts with the iron atom of heme through the quinoline nitrogen as shown in Figure 6B.

The binding of the most potent compound **14b** was also studied with μ-oxo dimers of heme at pH 5.8 using a standard procedure.[35] The stepwise addition of compound **14b** (0.3−16 μM) to a solution of μ-oxo dimer (10 μM) in 20 mM phosphate buffer at pH 5.8 resulted in a decrease in intensity of absorbance at 362 nm (Supporting Information, Figure S2). The Job's plot indicated a 1:1 stoichiometry for the most stable μ-oxo:**14b** complex (Supporting Information, Figure S2). The association constants calculated using HypSpec suggests that the binding of **14b** with μ-oxoheme (log K 5.84) is stronger than the monomeric heme (log K 4.63) and also is comparable to the standard CQ (log K 5.58). Thus, compound **14b** can be proposed to inhibit hemozoin formation by blocking the growing face of heme, which could be correlated with the observed antiplasmodial activity.

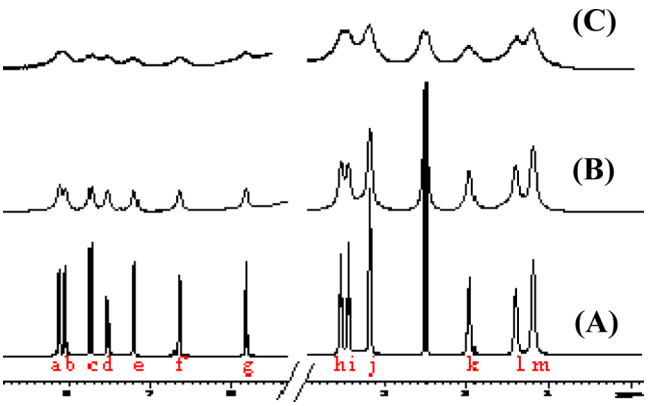

Figure 5. ^{1}H NMR spectral changes observed for **14b** after addition of increasing amounts of heme: (A) 0 mol %, (B) 10 mol, and (C) 30 mol in 40% DMSO:D_2O/D_2SO_4 (10 μL) [$\Delta\delta$ for peak: a = 0.021, b = 0.052, c = 0.015, d = 0.002, e = 0.026, f = 0.015, g = 0.010, h = 0.091, i = 0.063, j = 0.023, k = 0.008, l = 0.071, m = 0.013 ppm].

To further provide evidence for the inhibition of β-hematin formation by binding of **14b** with heme, polymerization of heme to β-hematin was conducted at 60 °C[53] in 4.5 M acetate buffer and the FT-IR of β-hematin shows bands at 1662 and 1209 cm^{-1}, characteristic of the iron carboxylate bonds. The disappearance of Fe-carboxylate bands upon binding to quinoline antimalarials has been established as proof-of-concept[54] to ascertain inhibition of β-hematin formation. The FT-IR spectra of the precipitate obtained upon incubation of heme with 1.2 equiv of **14b** using the literature-reported procedure[54] showed disappearance of peaks at 1662 and 1209 cm^{-1} assigned to β-hematin, indicating binding of heme with **14b** (Supporting Information, Figure S3). Further, the IR spectrum of the adduct of **14b** with heme is also significantly different from that of **14b** and heme itself (Supporting Information, Figures S4−S5).

DNA Binding Studies. 4-Aminoquinoline-based antimalarials such as **1** (CQ) interact with DNA in vitro through ionic interactions between the protonated nitrogen of the drug and the anionic phosphate groups of DNA in addition to the interactions between the aromatic nuclei of the drug with nucleotide bases,[55,56] thereby stabilizing the helical config-

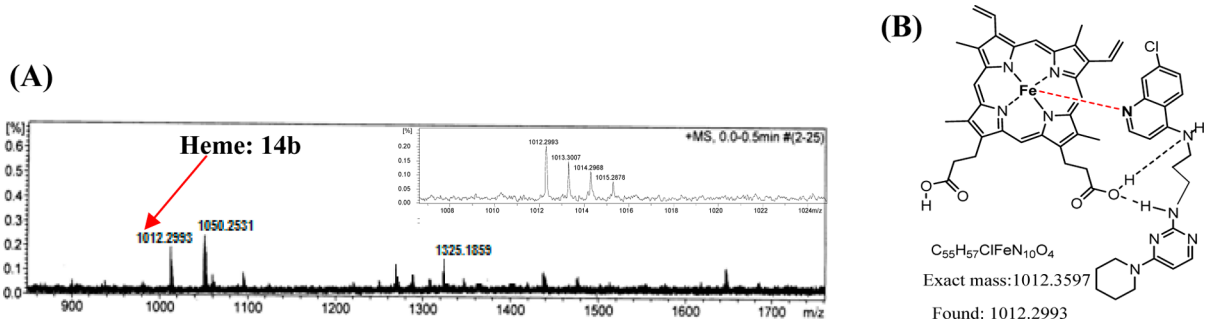

Figure 6. (A) The solution phase mass spectra of **14b** (5 μmol) upon addition of monomeric heme (5 μmol) in 40% aq DMSO solution (inset shows zoom between 1008 and 1024 Da); (B) proposed binding of heme with **14b**.

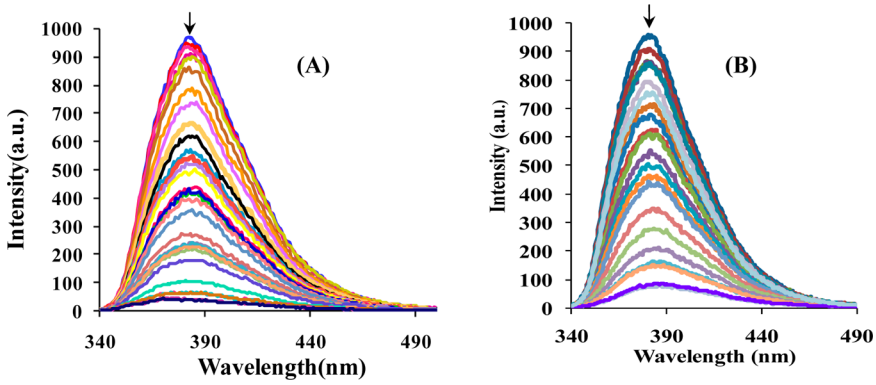

Figure 7. Fluorescence emission spectra (λ_{ex} = 330 nm, λ_{em} = 376 nm) of **14b** (17.1 μM) in buffered CH_3OH upon addition of increasing concentrations of (A) CT DNA (0.5−251 μM) and (B) pUC18 DNA (0.02−11.4 μM).

uration against thermal denaturation. Further, the buffering activity of **1** could additionally improve gene transfection efficiency by facilitating the DNA release from the endocytic pathways or by inhibiting lysosomal enzyme degradation.[57] Thus, the DNA binding ability of the new quinoline−pyrimidine hybrids was studied.

The addition of small increments of CT-DNA (0.5−251 μM) to the buffered methanolic solution of **14b** (17.1 μM) showed remarkable shifts in λ_{max} as well as in the absorption intensity. The characteristic quinoline ring absorption at 331 nm ($\pi \rightarrow \pi^*$) showed a hypochromic shift by 23% (Supporting Information, Figure S6) with a red-shift of ∼14 nm, suggesting an intercalative binding of **14b** with DNA base pairs,[58] which should also stabilize DNA and show an increment in the thermal melting temperature (T_m).[59] The melting temperature of CT DNA under our experimental conditions was 59.5 °C and it increases to 67.8 °C upon addition of **14b**, indicating the stabilization of the DNA duplex structure (Supporting Information, Table S9). Further, the derivative melting curve presented in Supporting Information, Figure S7 shows that the T_m of CT DNA upon addition of **14b** is comparable to that observed for the CQ.

Due to the fact that the malaria parasite exhibit unusually a higher AT content compared to human DNA,[60] the binding affinities of **14b** toward two DNA types having different nucleotide base composition were investigated using fluorescence spectrophotometery to allow the comparison of drug binding affinity specifically to GC vs AT-rich DNA. Addition of DNA (CT DNA and pUC18 DNA) to the buffered methanolic solution of **14b** (17.1 μM) induced a monotonous decrease of fluorescence intensity (Figure 7). Comparison of association constant estimated using HypSpec revealed that **14b** had a higher affinity for AT rich pUC18DNA.

■ CONCLUSIONS

In summary, we have reported the synthesis and systematic evaluation of structure−activity relationships of series of potent quinoline−pyrimidine hybrids. The in vitro evaluation of these hybrids against Dd2 and D10 strains of *P. falciparum* depicted activity in the nanomolar range. Among others, the compound **14b** exhibited the lowest IC_{50} value within the series against both the CQ^S and CQ^R strains of *P. falciparum*. Also, these hybrids exhibited high selectivity indices and low toxicity against the tested cell lines. Further, the binding capability of **14b** was evaluated with both heme and DNA to shed light on the mode of action of this class of hybrids.

■ EXPERIMENTAL PROCEDURES

General. All liquid reagents were dried/purified following recommended drying agents and/or distilled over 4 Å molecular sieves. THF was dried (Na-benzophenoneketyl) under nitrogen. ^1H NMR (300 and 400 MHz), ^{13}C (75 MHz and 100 MHz), HSQC, and HMBC NMR spectra were recorded in $CDCl_3$ and DMSO-d_6 on a multinuclear Jeol FT-AL-300 spectrometer and BrukerAvance II 400 spectrometer with chemical shifts being reported in parts per million (δ) relative to internal tetramethylsilane (TMS, δ 0.0, ^1H NMR) or chloroform ($CDCl_3$, δ 77.0, ^{13}C NMR). Mass spectra were recorded on a Bruker LC-MS MICROTOF II spectrometer. Elemental analysis was performed on FLASH EA 112 (Thermo Electron Corporation) analyzer, and the results are quoted in %. IR spectra were recorded on Perkin-Elmer FTIR-C92035 Fourier transform spectrometer in the range 400−4000 cm^{-1} using KBr pellets. For monitoring the progress of a reaction and for comparison purpose, thin layer chromatography (TLC) was performed on precoated aluminum sheets of Merck

($60F_{254}$, 0.2 mm) using an appropriate solvent system. The chromatograms were visualized under UV light. For column chromatography silica gel (60−120 mesh) was employed, and eluents were ethyl acetate/hexane or ethyl acetate/methanol mixtures. The pH measurements were performed with the Equip-Tronics digital pH meter model EQ 610. The HPLC system consisted of a Waters 2489 HPLC separations module equipped with Waters 2489 photodiode array detector, Waters 515 HPLC pump, and Empower software (Waters Corporation, Milford, MA, USA) for system control, data collection, and processing. Liquid chromatography was carried out using a Symmetry (4.6 mm × 75 mm), 3.5 μm C-18 reversed-phase column. The mobile phase consisted of premixed HPLC grade methanol and water in the varying ratio and degassed prior to operating under isocratic conditions at a flow rate of 0.4 mL/min with 20 μL standard sample injections. A calibration plot of the peak area versus compound concentration for each compound showed excellent linearity ($0.99 < r^2 < 1$) over the concentration range (0−10 μM) employed for the assays. The HPLC data was recorded at the absorption maximum (330 nm) for compounds **11**−**15** and 250 nm, the wavelength of maximum absorption (λ_{max}) for **13**. The retention time (t_R) is expressed in minutes (min). The purity of compounds **11**−**15** was evaluated by C,H,N analysis (FLASH EA 112 (Thermo Electron Corporation) analyzer) and HPLC methods (Supporting Information, Table S10). The purities of all the final compounds were confirmed to be ≥95% by combustion and HPLC analytical methods.

The steady state fluorescence experiments were carried out on Perkin-Elmer LS55 fluorescence spectrometer at ambient temperature. UV−visible spectral studies were conducted on Shimadzu 1601 PC spectrophotometer with a quartz cuvette (path length, 1 cm). The absorption spectra have been recorded between 1100 and 200 nm. The cell holder of the spectrophotometer was thermostatted at 25 °C for consistency in the recordings.

General Procedure for the Synthesis of 2,4-Dichloropyrimidine (8). Uracil (5 g, 0.04 mol) was suspended in phosphorus oxychloride ($POCl_3$) (25 mL) and heated at 105 °C for 6 h. Excess $POCl_3$ was removed under reduced pressure, and last traces were removed through azeotropic distillation with dry benzene (2 × 20 mL). The residue was then further purified by column chromatography (60−120 mesh silica) using hexane/EtOAc (92:8 v/v) as eluent to furnish **8** as white crystalline solid. Yield: 98%. ^{1}H (300 MHz, $CDCl_3$, 25 °C): δ 7.33 (d, J = 5.1 Hz, 1H, ArH), 8.52 (d, J = 5.1 Hz, 1H, ArH). ^{13}C NMR (75 MHz, $CDCl_3$, 25 °C): δ 120.3, 160.0, 161.07, and 162.6. Anal. Calcd for $C_4H_2N_2Cl_2$: C, 32.25; H, 1.35; N, 18.80. Found: C, 32.09; H, 1.27; N, 18.85. MS: m/z 147.9 (M^+).

General Procedure for the Synthesis of 11−13. The solution of appropriate aminoquinoline **9** or morpholine (0.021 mol) in dry THF (5 mL) was added to the stirred solution of **8** (0.018 mol) and potassium carbonate (0.09 mol) in dry THF (30 mL). The reaction mixture was stirred at room temperature for 48 h, and upon completion (TLC), the reaction mixture was filtered and the filtrate was concentrated under vacuum. The residue was purified by column chromatography using MeOH/EtOAc (**11** and **12**) or hexane/EtOAc (**13**) as eluent. Using this procedure, the following compounds were isolated.

*4-Chloro-2-[(7-chloroquinolin-4-ylamino)ethylamino]pyrimidine (**11a**).* Chromatographic eluent: MeOH/EtOAc (2:98 v/v). White solid. Yield: 58%. IR (KBr): ν_{max} 1579, 3055, 3275 cm^{-1}. ^{1}H (400 MHz, DMSO-d_6, 25 °C): δ 3.17 (m, 4H, CH_2), 6.46 (d, J = 6 Hz, 1H, ArH), 6.75 (d, J = 5.6 Hz, 1H, ArH), 7.47 (m, 2H, NH and ArH), 7.80 (s, 1H, ArH), 7.92 (d, J = 5.6 Hz, 1H, ArH), 8.11 (br, 1H, NH), 8.20 (m, 1H, ArH), 8.41 (d, J = 5.2 Hz, 1H, ArH). ^{13}C NMR (75 MHz, $CDCl_3$, 25 °C): δ 22.4, 37.7, 104.8, 154.7, 163.4, and 169.6. Anal. Calcd for $C_{15}H_{13}N_5Cl_2$: C, 53.91; H, 3.92; N, 20.96. Found: C, 53.75; H, 3.86; N, 20.91. MS: m/z 334 (M^+).

*4-Chloro-2-[(7-chloroquinolin-4-ylamino)propylamino]pyrimidine (**11b**).* Chromatographic eluent: MeOH/EtOAc (2:98 v/v). White solid. Yield: 65%. IR (KBr): ν_{max} 1596, 30,[38] 3111 cm^{-1}. ^{1}H (300 MHz, DMSO-d_6, 25 °C): δ 2.00 (m, 2H, CH_2), 3.47 (m, 4H, CH_2), 6.44 (m, 2H, ArH), 7.05 (br, 1H, NH), 7.35 (m, 1H, ArH), 7.61 (br, 1H, NH), 7.85 (d, J = 1.8, 2H, ArH), 8.02 (m, 1H, ArH), 8.42 (d, J = 5.4 Hz, 1H, ArH). ^{13}C NMR (100 MHz, DMSO-d_6, 25 °C): δ 26.9, 37.8, 40.1, 98.5, 104.9, 117.2, 124.4, 126.4, 133.9, 147.7, 150.6, 154.9, 159.9, and 163.4. Anal. Calcd for $C_{16}H_{15}N_5Cl_2$: C, 55.10; H, 4.31; N, 20.11. Found: C, 54.99; H, 4.38; N, 20.01. MS: m/z 348 (M^+).

*4-Chloro-2-[(7-chloroquinolin-4-ylamino)butylamino]pyrimidine (**11c**).* Chromatographic eluent: MeOH/EtOAc (1:99 v/v). White solid. Yield: 56%. IR (KBr): ν_{max} 1581, 2928, 3253 cm^{-1}. ^{1}H (300 MHz, DMSO-d_6, 25 °C): δ 1.61 (m, 4H, CH_2), 3.25 (m, 2H, CH_2), 6.44 (m, 1H, ArH), 6.60 (m, 1H, ArH), 7.30 (br, 1H, NH), 7.41 (m, 1H, ArH), 7.62 (br, 1H, NH), 7.75 (m, 1H, ArH), 8.19 (m, 1H, ArH), 8.34 (m, 1H, ArH). ^{13}C NMR (75 MHz, DMSO-d_6, 25 °C): δ 29.5, 99.2, 109.8, 117.8, 124.6, 124.8, 127.3, 134.2, 148.7, 151.0, 151.7, 160.8, and 162.9. Anal. Calcd for $C_{17}H_{17}N_5Cl_2$: C, 56.36; H, 4.73; N, 19.23. Found: C, 56.42; H, 4.69; N, 19.05. MS: m/z 362 (M^+).

*4-Chloro-2-[(7-chloroquinolin-4-ylamino)heptylamino]pyrimidine (**11d**).* Chromatographic eluent: EtOAc. Yellow solid. Yield: 65%. IR (KBr): 1612, 2930, 3415 cm^{-1}. ^{1}H (400 MHz, DMSO-d_6, 25 °C): δ 1.33 (m, 6H, CH_2), 1.49 (m, 2H, CH_2), 1.67 (m, 2H, CH_2), 3.24 (m, 4H, CH_2), 6.47 (d, J = 5.5 Hz, 1H, ArH),6.85 (d, J = 6.5 Hz, 1H, ArH), 7.39 (m, 1H, ArH), 7.85 (d, J = 4.6 Hz, 1H, ArH),7.95 (m, 1H, ArH), 8.52 (d, J = 6.3 Hz, 1H, ArH),8.72 (d, J = 9.0 Hz, 1H, ArH),8.82 (d, J = 3.6 Hz, 1H, Ar), 9.66 (br, 1H, NH). ^{13}C NMR (100 MHz, DMSO-d_6, 25 °C): δ 26.2, 27.7, 28.3, 43.0, 98.7, 100.1, 104.9, 115.3, 118.9, 125.8, 126.6, 137.8, 138.4, 142.1, 151.4, 154.9, 159.7, 163.3, and 164.3. Anal. Calcd for $C_{20}H_{23}N_5Cl_2$: C, 59.41; H, 5.73; N, 17.32. Found: C, 59.46; H, 5.79; N, 17.33. MS: m/z 404 (M^+).

*4-Chloro-2-[(7-chloroquinolin-4-ylamino)octylamino]pyrimidine (**11e**).* Chromatographic eluent: EtOAc. Yellow solid. Yield: 65%. IR (KBr): ν_{max} 1576, 2930, 3292 cm^{-1}. ^{1}H (400 MHz, DMSO-d_6, 25 °C): δ 1.34 (m, 8H, CH_2), 1.48 (m, 2H, CH_2), 1.64 (m, 2H, CH_2), 3.18 (m, 2H, CH_2), 3.23 (m, 2H, CH_2), 6.42 (m, 2H, ArH), 7.28 (br, 1H, NH), 7.43 (dd, $J_{1,2}$ = 8.9 Hz, $J_{1,3}$ = 2.2 Hz, 1H, ArH), 7.78 (d, J = 2.2 Hz, 1H, ArH), 7.86 (m, 2H, ArH and NH), 8.27 (d, J = 9.0 Hz, 1H, ArH), 8.38 (d, J = 5.4 Hz, 1H, Ar). ^{13}C NMR (100 MHz, DMSO-d_6, 25 °C): δ 26.6, 28.1, 29.0, 42.6, 48.9, 98.9, 105.3, 117.7, 124.4, 127.5, 134.0, 149.2, 150.6, 152.2, 155.5, 160.3, and 163.7. Anal. Calcd for $C_{21}H_{25}N_5Cl_2$: C, 60.29; H, 6.02; N, 16.74. Found: C, 60.14; H, 6.43; N, 16.83. MS: m/z 418 (M^+).

*4-Chloro-2-[(7-chloroquinolin-4-ylamino)decylamino]pyrimidine (**11f**).* Chromatographic eluent: hexane/EtOAc (85:15 v/v). Yellow solid. Yield: 60%. IR (KBr): ν_{max} 1599, 2919, 3260 cm^{-1}. ^{1}H (400 MHz, DMSO-d_6, 25 °C): δ 1.27 (m, 12H, CH_2), 1.54 (m, 4H, CH_2), 3.15 (m, 4H, CH_2), 6.48 (m, 2H, ArH), 6.66 (dd, J = 5.6 Hz, 1H, ArH), 7.55 (d, $J_{1,2}$ = 8.8 Hz, 1H, ArH), 7.71 (br, 1H, NH), 7.86 (s, 1H, ArH), 8.42 (d, J = 9.0 Hz, 1H, ArH), 8.46 (d, J = 5.6 Hz, 1H, ArH). ^{13}C NMR (100 MHz, DMSO-d_6, 25 °C): δ 21.0, 26.3, 42.5, 98.5, 100.3, 104.9, 117.0, 124.4, 125.7, 134.2, 151.0, 155.1, 157.6, 159.9, 163.3, and 172.0. Anal. Calcd for $C_{23}H_{29}N_5Cl_2$: C, 61.88; H, 6.55; N, 15.69. Found: C, 61.96; H, 6.37; N, 15.63. MS: m/z 446 (M^+).

*4-Chloro-2-[(7-chloroquinolin-4-ylamino)dodecylamino]pyrimidine (**11g**).* Chromatographic eluent: hexane/EtOAc (82:18 v/v). Yellow solid. Yield: 58%. IR (KBr): ν_{max} 1596, 2920, 3259 cm^{-1}. ^{1}H (400 MHz, DMSO-d_6, 25 °C): δ 1.32 (m, 16H, CH_2), 1.53 (m, 4H, CH_2), 3.27 (m, 4H, CH_2), 6.49 (m, 2H, ArH), 6.68 (d, J = 5.1 Hz, 1H, ArH), 7.43 (br, 1H, NH), 7.50 (dd, $J_{1,2}$ = 8.9 Hz, $J_{1,3}$ = 2.2 Hz, 1H, ArH), 7.72 (br, 1H, NH), 7.83 (s, 1H, ArH), 8.34 (d, J = 9.0 Hz, 1H, ArH), 8.44 (d, J = 5.5 Hz, 1H, ArH). ^{13}C NMR (100 MHz, DMSO-d_6, 25 °C): δ 26.3, 28.3, 28.6, 28.9, 42.3, 104.9, 117.3, 124.0, 133.4, 155.2, 159.9, and 163.3. Anal. Calcd for $C_{25}H_{33}N_5Cl_2$: C, 63.28; H, 7.01; N, 14.76. Found: C, 63.35; H, 7.07; N, 14.81. MS: m/z 474 (M^+).

*4-Chloro-2-[(7-chloroquinolin-4-ylamino)propoxy]pyrimidine (**11h**).* Chromatographic eluent: EtOAc. White solid. Yield: 97%. IR (KBr): ν_{max} 1576, 2962, 3215 cm^{-1}. ^{1}H (400 MHz, DMSO-d_6, 25 °C): δ 2.19 (quin, J = 5.1 Hz, 2H, CH_2), 3.49 (q, J = 6.6 Hz, 2H, CH_2), 4.51 (t, J = 6.3 Hz, 2H, CH_2), 6.57 (d, J = 5.5 Hz, 1H, ArH), 7.06 (d, J = 5.7 Hz, 1H, ArH), 7.43 (br, 1H, NH), 7.51 (dd, $J_{1,2}$ = 9 Hz, $J_{1,3}$ = 2.2 Hz,1H, ArH), 7.84 (d, J = 2.4 Hz, 1H, ArH), 8.32 (d, J = 9.0 Hz, 1H, ArH), 8.45 (d, J = 5.4 Hz, 1H, ArH), 8.52 (d, J = 5.8 Hz, 1H, ArH). ^{13}C NMR (100 MHz, DMSO-d_6, 25 °C): δ 27.2, 65.8, 99.2, 108.0,

124.6, 127.9, and 160.3. Anal. Calcd for $C_{16}H_{14}N_5Cl_2O$: C, 55.03; H, 4.04; N, 16.04. Found: C, 55.13; H, 4.18; N, 16.21. MS: m/z 348 ($M^+ - 1$).

*2-Chloro-4-[(7-chloroquinolin-4-ylamino)ethylamino] pyrimidine (**12a**).* Chromatographic eluent: EtOAc. White solid. Yield: 25%. IR (KBr): ν_{max}, 1583, 3064, 3252 cm^{-1}. ^1H (400 MHz, DMSO-d_6, 25 °C): δ 3.34 (m, 4H, CH_2), 6.68 (m, 2H, ArH), 7.42 (m, 1H, ArH), 7.77 (s, 1H, ArH), 7.88 (d, J = 5.6 Hz, 1H, ArH), 8.00 (br, 1H, NH), 8.17 (m, 2H, ArH), 8.39 (d, J = 4.2 Hz, 1H, ArH). ^{13}C NMR (75 MHz, $CDCl_3$, 25 °C): δ 29.5, 99.2, 109.8, 117.7, 124.6, 127.3, 134.2, 148.7, 151.0, 160.7, and 162.8. Anal. Calcd for $C_{15}H_{13}N_5Cl_2$: C, 53.91; H, 3.92; N, 20.96. Found: C, 53.95; H, 4.07; N, 20.80. MS: m/z 334 (M^+).

*2-Chloro-4-[(7-chloroquinolin-4-ylamino)propylamino]-pyrimidine (**12b**).* Chromatographic eluent: EtOAc. White solid. Yield: 25%. IR (KBr): ν_{max}1670, 3111, 3201 cm^{-1}. ^1H (300 MHz, $CDCl_3$, 25 °C): δ 2.01 (m, 2H, CH_2), 3.44 (m, 2H, CH_2), 3.60 (m, 2H, CH_2), 6.26 (br, 1H, NH), 6.57 (d, J = 5.7 Hz, 2H, ArH), 6.72 (br, 1H, NH), 7.36 (m, 1H, ArH), 7.92 (m, 2H, ArH), 8.15 (d, J = 5.1 Hz, 1H, ArH), 8.40 (d, J = 5.7 Hz, 1H, ArH). ^{13}C NMR (100 MHz, DMSO-d_6, 25 °C): δ 27.2, 38.5, 39.3, 98.6, 108.7, 117.3, 117.4, 124.0, 127.4, 133.3, 148.9, 149.9, 150.0, 151.8, 159.9, and 162.3. Anal. Calcd for $C_{16}H_{15}N_5Cl_2$: C, 55.10; H, 4.31; N, 20.11. Found: C, 55.24; H, 4.35; N, 20.08. MS: m/z 348 (M^+).

*2-Chloro-4-[(7-chloroquinolin-4-ylamino)octylamino]pyrimidine (**12c**).* Chromatographic eluent: EtOAc. Yellow solid. Yield: 30%. IR (KBr): ν_{max} 1579, 2953, 3250 cm^{-1}. ^1H (400 MHz, DMSO-d_6, 25 °C): δ 1.36 (m, 8H, CH_2), 1.49 (m, 2H, CH_2), 1.65 (m, 2H, CH_2), 3.24 (m, 4H, CH_2), 6.44 (m, 2H, ArH), 6.63 (dd, $J_{1,2}$ = 9.0 Hz, $J_{1,3}$ = 2.2 Hz, 1H, ArH), 7.29 (br, 1H, NH), 7.43 (d, J = 6.7 Hz, 1H, ArH), 7.67 (br, 1H, NH), 7.77 (d, J = 2.2 Hz, 1H, ArH), 8.27 (d, J = 9.0 Hz, 1H, ArH), 8.39 (d, J = 5.4 Hz, 1H, Ar). ^{13}C NMR (100 MHz, $CDCl_3$, 25 °C): δ 26.6, 28.7, 29.0, 29.1, 29.3, 41.4, 43.2, 98.9, 109.7, 121.0, 125.3, 151.3, 159.0, and 163.6. Anal. Calcd for $C_{21}H_{25}N_5Cl_2$: C, 60.29; H, 6.02; N, 16.74. Found: C, 60.42; H, 6.12; N, 16.49. MS: m/z 418 (M^+).

*4-Chloro-2-morpholinopyrimidine (**13**).* Chromatographic eluent: hexane/EtOAc (90:10 v/v). White solid. Yield: 98%. IR (KBr): ν_{max} 1589, 2972, 3091 cm^{-1}. ^1H (300 MHz, $CDCl_3$, 25 °C): δ 3.64 (m, 4H, CH_2), 3.76 (m, 4H, CH_2), 6.37 (m, 1H, ArH), 8.06 (m, 1H, ArH). ^{13}C NMR (75 MHz, $CDCl_3$, 25 °C): δ 29.6, 44.2, 66.3, 101.0, and 157.5. Anal. Calcd for $C_8H_{10}N_3OCl$: C, 48.13; H, 5.05; N, 21.05. Found: C, 48.07; H, 5.19; N, 21.17. MS: m/z 200.0 (M^++1).

General Procedure for the Synthesis of 14−15. To the stirred solution of compound **11b** or **12b** (0.055 mol) and potassium carbonate (0.25 mol) in dry acetonitrile (20 mL), an appropriate amine (morpholine/piperidine/piperazine/pyrrolidine) (0.018 mol) was added. The reaction mixture was refluxed for 2 h, and upon completion (TLC), the crude product was filtered and recrystallized from DCM/hexane. The following compounds were isolated.

*4-Morpholinyl-2-[(7-chloroquinolin-4-ylamino)propylamino]-pyrimidine (**14a**).* White solid. Yield: 97%. IR (KBr): ν_{max} 1586, 2962, 3376 cm^{-1}. ^1H (400 MHz, $CDCl_3$, 25 °C): δ 2.07 (m, 2H, CH_2), 3.45 (m, 2H, CH_2), 3.56 (m, 2H, CH_2), 3.70 (m, 8H, CH_2), 4.78 (br, 1H, NH), 5.13 (br, 1H, NH), 5.71(d, J = 5.7 Hz, 1H, ArH), 6.40 (d, J = 5.4 Hz, 1H, ArH), 7.34 (dd, $J_{1,2}$ = 8.9 Hz, $J_{1,3}$ = 2 Hz,1H, ArH), 7.54 (d, J = 8.7 Hz, 1H, ArH), 7.89 (d, J = 5.4 Hz, 1H, ArH), 7.96 (d, J = 2.1 Hz, 1H, ArH), 8.51 (d, J = 5.1 Hz, 1H, ArH). ^{13}C NMR (75 MHz, $CDCl_3$, 25 °C): δ 28.5, 29.7, 38.7, 41.1, 44.3, 66.8, 98.9, 117.1, 121.1, 125.5, 128.4, 128.6, 129.7, 135.0, 148.8, 149.8, 151.7, 156.0, 161.7, and 162.8. Anal. Calcd for $C_{20}H_{23}N_6Cl$ O: C, 60.22; H, 5.81; N, 21.07. Found: C, 60.18; H, 5.98; N, 21.24. MS: m/z 398 (M^+).

*4-Piperidinyl-2-[(7-chloroquinolin-4-ylamino)propylamino]-pyrimidine (**14b**).* Yellow solid. Yield: 98%. IR (KBr): ν_{max} 1580, 2923, 3401 cm^{-1}. ^1H (400 MHz, $CDCl_3$, 25 °C): δ 1.51 (m, 4H, CH_2), 2.05 (m, 4H, CH_2), 3.43 (m, 2H, CH_2), 3.55 (m, 2H, CH_2), 3.70 (m, 4H, CH_2),4.91 (br, 1H, NH), 5.40 (br, 1H, NH), 5.63 (d, J = 5.7 Hz, 1H, ArH), 6.38 (d, J = 5.4 Hz, 1H, ArH), 7.30 (dd, $J_{1,2}$ = 8.8 Hz, $J_{1,3}$ = 1.9 Hz,1H, ArH), 7.56 (d, J = 8.9 Hz, 1H, ArH), 7.86 (d, J = 5.7 Hz, 1H, ArH), 7.92 (s, 1H, ArH), 8.49 (d, J = 5.3 Hz, 1H, ArH). ^{13}C NMR (75 MHz, $CDCl_3$, 25 °C): δ 24.9, 25.7, 28.5, 38.7, 41.0, 44.8, 98.9, 117.1, 121.0, 125.3, 128.4, 135.0, 148.8, 149.6, 151.7, 156.1, 161.6, and 162.8. Anal. Calcd for $C_{20}H_{23}N_6Cl$ O: C, 60.22; H, 5.81; N, 21.07. Found: C, 60.36; H, 5.92; N, 21.14. MS: m/z 397 (M^+).

*4-Piprazinyl-2-[(7-chloroquinolin-4-ylamino)propylamino]-pyrimidine (**14c**).* White solid. Yield: 97%. IR (KBr): ν_{max} 1567, 3088, 3403 cm^{-1}. ^1H (400 MHz, DMSO-d_6, 25 °C): δ 1.27 (m, 2H, CH_2), 3.33 (m, 2H, CH_2), 3.50 (m, 4H, CH_2), 3.66 (m, 4H, ArH), 5.78 (d, J = 5.7 Hz, 1H, ArH), 6.42 (d, J = 5.5 Hz, 1H, ArH), 6.85 (br, 1H, ArH), 7.24 (br, 1H, NH), 7.34 (dd, $J_{1,2}$ = 9 Hz, $J_{1,3}$ = 2.1 Hz,1H, ArH), 7.74 (m, 2H, ArH), 7.75 (m, 1H, ArH), 8.21 (d, J = 9 Hz, 1H, ArH), 8.38 (d, J = 5.4 Hz, 1H, ArH). ^{13}C NMR (75 MHz, $CDCl_3$, 25 °C): δ 25.4, 33.2, 39.6, 98.7, 123.4, 117.1, 124.2, 125.3, and 161.2. Anal. Calcd for $C_{20}H_{24}N_7Cl$: C, 60.37; H, 6.08; N, 24.64. Found: C, 60.49; H, 5.95; N, 24.53. MS: m/z 398 (M^+ + 1).

*4-Pyrolidinyl-2-[(7-chloroquinolin-4-ylamino)propylamino]-pyrimidine (**14d**).* Yellow solid. Yield: 89%. IR (KBr): ν_{max} 1582, 2957, 3336 cm^{-1}. ^1H (400 MHz, $CDCl_3$, 25 °C): δ 1.74 (m, 2H, CH_2), 2.04 (m, 4H, CH_2), 3.33 (m, 2H, CH_2), 3.45 (m, 6H, CH_2), 5.52 (br, 1H, NH), 5.65 (m, 1H, ArH), 5.98 (br, 1H, NH), 6.39 (d, J = 5.4 Hz, 1H, ArH), 7.29 (dd, $J_{1,2}$ = 9 Hz, $J_{1,3}$ = 1.9 Hz, 1H, ArH), 7.61 (m, 1H, ArH), 7.83 (m, 1H, ArH), 7.93 (m, 1H, ArH), 8.49 (d, J = 5.3 Hz, 1H, ArH). ^{13}C NMR (75 MHz, $CDCl_3$, 25 °C): δ 23.2, 39.1, 28.4, 29.6, 36.7, 38.6, 41.1, 93.5, 98.8, 117.1, 121.2, 125.1,128.3, 134.8, 148.8, 149.8, 151.6, 155.6, 160.1, 162.7, and 170.5. Anal. Calcd for $C_{20}H_{23}N_6Cl$: C, 62.74; H, 6.05; N, 21.95. Found: C, 62.64; H, 6.23; N, 21.76. MS: m/z 383 (M^++1).

*2-Morpholinyl-4-[(7-chloroquinolin-4-ylamino)propylamino]-pyrimidine (**15a**).* White solid. Yield: 98%. IR (KBr): ν_{max} 1586, 2955, 3245 cm^{-1}. ^1H (400 MHz, $CDCl_3$, 25 °C): δ 1.94 (m, 2H, CH_2), 3.42 (m, 2H, CH_2), 3.57 (m, 6H, CH_2), 3.70 (m, 4H, CH_2), 4.97 (br, 1H, NH), 5.91 (d, J = 6.0 Hz, 1H, ArH), 6.40 (d, J = 5.4 Hz, 1H, ArH), 7.34 (dd, $J_{1,2}$ = 8.7 Hz, $J_{1,3}$ = 2.1 Hz,1H, ArH), 7.81 (d, J = 9 Hz, 1H, ArH), 7.95 (m, 2H, ArH), 8.49 (d, J = 5.4 Hz, 1H, ArH). ^{13}C NMR (100 MHz, $CDCl_3$, 25 °C): δ 28.9, 38.3, 39.7, 44.0, 46.4, 66.5, 68.0, 93.8, 98.7, 117.6, 121.7, 125.0, 128.5, 134.7, 149.2, 150.1, 151.9, 156.3, 162.3, and 162.7. Anal. Calcd for $C_{20}H_{23}N_6Cl$ O: C, 60.22; H, 5.81; N, 21.07. Found: C, 60.12; H, 5.59; N, 21.26. MS: m/z 398 (M^+).

*2-Piperidinyl-4-[(7-chloroquinolin-4-ylamino)propylamino]-pyrimidine (**15b**).* Yellow solid. Yield: 94%. IR (KBr): ν_{max} 1583, 2976, 3310 cm^{-1}. ^1H (400 MHz, $CDCl_3$, 25 °C): δ 1.6 (m, 4H, CH_2), 1.93 (m, 2H, CH_2), 3.31 (m, 2H, CH_2), 3.44 (m, 2H, CH_2), 3.54 (m, 4H, CH_2), 3.70 (m, 2H, CH_2), 5.64 (br, 1H, NH), 5.93 (dd, $J_{1,2}$ = 17.2 Hz, $J_{1,3}$ = 6.2 Hz, 1H, ArH), 6.38 (d, J = 5.5 Hz, 1H, ArH), 7.33 (dd, $J_{1,2}$ = 8.8 Hz, $J_{1,3}$ = 2 Hz, 1H, ArH), 7.86 (m,2H, ArH), 7.91 (d, J = 2.4 Hz, 1H, ArH), 8.47 (m, 1H, ArH). ^{13}C NMR (75 MHz, $CDCl_3$, 25 °C): δ 24.9, 25.7, 28.5, 38.7, 41.0, 44.8, 98.9, 117.1, 121.0, 125.3, 128.4, 135.0, 148.8, 149.6, 151.7, 156.1, 161.6, and 162.8. Anal. Calcd for $C_{20}H_{23}N_6Cl$ O: C, 60.22; H, 5.81; N, 21.07. Found: C, 60.03; H, 6.08; N, 21.38. MS: m/z 397 (M^+).

In Vitro Antimalarial Activity Assay. The test samples were tested in triplicate on one or two separate occasions against chloroquine sensitive (CQ^S) D10 and chloroquine-resistant (CQ^R) Dd2 strains of *P. falciparum*. Continuous in vitro cultures of asexual erythrocyte stages of *P. falciparum* were maintained using a modified method of Trager and Jensen.[61] Quantitative assessment of antiplasmodial activity in vitro was determined via the parasite lactate dehydrogenase assay using a modified method described by Makler.[62] The test samples were prepared to a 20 mg/mL stock solution in 100% DMSO. Stock solutions were stored at −20 °C. Further dilutions were prepared on the day of the experiment. Chloroquine diphosphate (CQ) (Sigma), artesunate (Sigma), and an in-house control MMV390048 were used as the reference drugs in all experiments. A full dose−response was performed for all compounds to determine the concentration inhibiting 50% of parasite growth (IC_{50} value). Test samples were tested at a starting concentration of 10 μg/mL, which was then serially diluted 2-fold in complete medium to give 10 concentrations, with the lowest concentration being 0.02 μg/mL. The same dilution technique was used for all samples. Reference drugs were tested at a starting concentration of 1000 ng/mL. Several

compounds were tested at a starting concentration of 1000 ng/mL. The highest concentration of solvent to which the parasites were exposed to had no measurable effect on the parasite viability (data not shown). The IC_{50} values were obtained using a nonlinear dose–response curve fitting analysis via Graph Pad Prism v.4.0 software.

Cytotoxicity and Antiviral Activity Assays. Cytotoxicity was determined by exposing different concentrations of the samples to Vero, HEL, HeLa, CrFK, and MDCK cells.[35] The antiviral assays were based on inhibition of virus-induced cytopathicity in HEL (herpes simplex virus type 1 (HSV-1), HSV-2 (G), vaccinia virus, and vesicular stomatitis virus), Vero (parainfluenza-3, reovirus-1, Coxsackie B4, and Punta Toro virus), HeLa (vesicular stomatitis virus, Coxsackie virus B4, and respiratory syncytial virus), CrFK (FIPV and FHV), and MDCK (influenza A (H1N1, H3N2) and B virus) cell cultures. Confluent cell cultures in microtiter 96-well plates were inoculated with 100 cell culture inhibitory dose-50 ($CCID_{50}$) of virus (1 $CCID_{50}$ being the virus dose to infect 50% of the cell cultures) in the presence of varying concentrations of the test compounds. Viral cytopathicity was recorded as soon as it reached completion in the control virus-infected cell cultures that were not treated with the test compounds.[35] The cytotoxicity was microscopically determined or examined with the viability staining (MTT) method.

■ ASSOCIATED CONTENT

Supporting Information

Procedure for determination of aqueous solubility, partition coefficient, acid dissociation constants, and binding constants with heme and DNA, spectral data of **11b**/**12b** and **14a**/**15a**, crystal data for **14a**, cytotoxicity and antiviral activity results and FT-IR spectra of heme, β-hematin, and heme:**14b** adduct. This material is available free of charge via the Internet at http://pubs.acs.org

■ AUTHOR INFORMATION

Corresponding Author

*Phone: +91 183 2258853; +91 183 2258802-09 ext 3508. Fax: +91 183 2258819/20. E-mail: kamaljit19in@yahoo.co.in.

Notes

The authors declare no competing financial interest.

■ ACKNOWLEDGMENTS

K.S. gratefully acknowledges financial assistance from CSIR, New Delhi (project 01(2364)/10/EMR-II), and UGC, New Delhi, for Special Assistance Programme (SAP). Thanks are due to the Sophisticated Instrumentation Centre, IIT Indore, for single crystal X-ray analysis. H.K. thanks CSIR, New Delhi (F. no. 09/254 (0195)/2009-EMR-I) for a senior research fellowship. J.B. thanks KU Leuven for financial support (GOA 10/14).The South African Research Chairs Initiative of the Department of Science and Technology, the South African Medical Research Council, and the University of Cape Town are gratefully acknowledged for financial support (K.C.).

■ ABBREVIATIONS USED

PfCRT, *Plasmodium falciparum* chloroquine resistance transporter; DV, digestive vacuole; CT-DNA, calf thymus DNA; ASN, artesunate; FPIX, ferriprotoporphyrin IX; HSQC, heteronuclear multiple quantum correlation; HMBC, heteronuclear multiple bond correlation

■ REFERENCES

(1) Christoph, H.; Salas, P. F.; Patrick, B. O.; de Kock, C.; Smith, P. J.; Adam, M. J.; Orvig, C. 1,2-Disubstituted ferrocenyl carbohydrate Chloroquine conjugates as potential antimalarial agents. *Dalton Trans.* **2012**, *41*, 6431–6442.

(2) *World Malaria Report*; WHO: Geneva, December 2012.

(3) *Medical Surveillance Monthly Report*; U.S. Armed Forces Health Surveillance Center: Aberdeen, MD, January 2013; Vol. *20*, no. 1.

(4) The Global Malaria Epidemic. *U.S. Global Health Policy Fact Sheet*; The Henry J. Kaiser Family Foundation: Menlo Park, CA; March 2013.

(5) Zhang, H.; Paguio, M.; Roepe, P. D. The antimalarial drug resistance protein *Plasmodium falciparum* chloroquine resistance transporter binds chloroquine. *Biochemistry* **2004**, *43*, 8290–8296.

(6) Bray, P. G.; Martin, R. E.; Tilley, L.; Ward, S. A.; Kirk, K.; Fidock, D. A. Defining the role of PfCRT in *Plasmodium falciparum* chloroquine resistance. *Mol. Microbiol.* **2005**, *56*, 323–333.

(7) Fidock, D. A.; Nomura, T.; Talley, A. K.; Cooper, R. A.; Dzekunov, S. M.; Ferdig, M. T.; Ursos, L. M.; Sidhu, A. B.; Naude, B.; Deitsch, K. W.; Su, X. Z.; Wootton, J. C.; Roepe, P. D.; Wellems, T. E. Mutations in the *P. falciparum* digestive vacuole transmembrane protein PfCRT and evidence for their role in chloroquine resistance. *Mol. Cell* **2000**, *6*, 861–871.

(8) Krogstad, D. J.; Gluzman, I. Y.; Kyle, D. E.; Oduola, A. M.; Martin, S. K.; Milhous, W. K.; Schlesinger, P. H. Efflux of chloroquine from *Plasmodium falciparum*: mechanism of chloroquine resistance. *Science* **1987**, *238*, 1283–1285.

(9) Martin, R. E.; Marchetti, R. V.; Cowan, A. I.; Howitt, S. M.; Broer, S.; Kirk, K. Chloroquine transport via the malaria parasite's chloroquine resistance transporter. *Science* **2009**, *325*, 1680–1682.

(10) Foley, M.; Tilley, L. Quinoline antimalarials: mechanisms of action and resistance. *Int. J. Parasitol.* **1997**, *27*, 231–240.

(11) Sharma, A.; Mishra, N. C. Inhibition of a protein tyrosine kinase activity in *Plasmodium falciparum* by chloroquine. *Indian J. Biochem. Biophys.* **1999**, *36*, 299–304.

(12) Ciak, J.; Hahn, F. E. Chloroquine: mode of action. *Science* **1996**, *151*, 347–349.

(13) Jagt, D. L. V.; Hunsakker, L. A.; Campos, N. M. Characterization of a hemoglobin-degrading, low molecular weight protease from Plasmodium falciparum. *Mol. Biochem. Parasitol.* **1986**, *18*, 389–400.

(14) Kubo, M.; Hostetler, K. Y. Mechanism of cationic amphiphilic drug inhibition of purified lysosomal phospholipase A1. *Biochemistry* **1985**, *24*, 6515–6520.

(15) Kaur, K.; Jain, M.; Reddy, R. P.; Jain, R. Quinolines and structurally related heterocycles as antimalarials. *Eur. J. Med. Chem.* **2010**, *45*, 3245–3264.

(16) Muregi, F. W.; Ishih, A. Next-generation antimalarial drugs: hybrid molecules as a new strategy in drug design. *Drug Dev. Res.* **2010**, *71*, 20–32.

(17) Chauhan, S. S.; Sharma, M.; Chauhan, P. M. S. Trioxaquines: hybrid molecules for the treatment of malaria. *Drug News Perspect.* **2010**, *23*, 632–646.

(18) Walsh, J. J.; Coughlan, D.; Heneghan, N.; Gaynor, C.; Bell, A. A novel artemisinin–quinine hybrid with potent antimalarial activity. *Bioorg. Med. Chem. Lett.* **2007**, *17*, 3599–3602.

(19) Dechy-Cabaret, O.; Benoit-Vical, F.; Robert, A.; Meunier, B. Preparation and antimalarial activities of "trioxaquines", new modular molecules with a trioxane skeleton linked to a 4-aminoquinoline. *ChemBioChem* **2000**, *1*, 281–283.

(20) Vical, F. B.; Lelièvre, J.; Berry, A.; Deymier, C.; Dechy-Cabaret, O.; Cazelles, J.; Loup, C.; Robert, A.; Magnaval, J.-F.; Meunier, B. Trioxaquines are new antimalarial agents active on all erythrocytic forms, including gametocytes. *Antimicrob. Agents Chemother.* **2007**, *51*, 1463–1472.

(21) Coslédan, F.; Fraisse, L.; Pellet, A.; Guillou, F.; Mordmüller, B.; Kremsner, P. G.; Moreno, A.; Mazier, D.; Maffrand, J.-P.; Meunier, B. Selection of a trioxaquine as an antimalarial drug candidate. *Proc. Natl. Acad. Sci. U. S. A.* **2008**, *105*, 17579–17584.

(22) Pérez, B. C.; Teixeira, C.; Albuquerque, I. S.; Gut, J.; Rosentha, P. J.; Gomes, J. R. B.; Prudêncio, M.; Gomes, P. *N*-Cinnamoylated chloroquine analogues as dual-stage antimalarial leads. *J. Med. Chem.* **2013**, *56*, 556–567.

(23) Salas, P. F.; Herrmann, C.; Cawthray, J. F.; Nimphius, C.; Kenkel, A.; Chen, J.; de Kock, C.; Smith, P. J.; Patrick, B. O.; Adam, M. J.; Orvig, C. Structural characteristics of chloroquine-bridged ferrocenophane analogues of ferroquine may obviate malaria drug-resistance mechanisms. *J. Med. Chem.* **2013**, *56*, 1596−1613.
(24) Chauhan, K.; Sharma, M.; Saxena, J.; Singh, S. V.; Trivedi, P.; Srivastava, K.; Puri, S. K.; Saxena, J. K.; Chaturvedi, V.; Chauhan, P. M. S. Synthesis and biological evaluation of a new class of 4-aminoquinoline-rhodanine hybrid as potent anti-infective agents. *Eur. J. Med. Chem.* **2013**, *62*, 693−704.
(25) Pal, C.; Sarkar, S.; Mazumder, S.; Adhikari, S.; Bandyopadhyay, U. Synthesis and biological evaluation of primaquine−chloroquine twin drug: a novel heme-interacting molecule prevents free heme and hydroxyl radical-mediated protein degradation. *MedChemComm* **2013**, *4*, 731−736.
(26) Kumar, A.; Srivastava, K.; Chauhan, P. M. S. Synthesis and bioevaluation of hybrid 4-aminoquinoline triazines as a new class of antimalarial agents. *Bioorg. Med. Chem. Lett.* **2008**, *18*, 6530−6533.
(27) Chiyanzu, I.; Clarkson, C.; Smith, P. J.; Lehman, J.; Gut, J.; Rosenthal, P. J.; Chibale, K. Design, synthesis and anti-plasmodial evaluation in vitro of new 4-aminoquinoline isatin derivatives. *Bioorg. Med. Chem.* **2005**, *13*, 3249−3261.
(28) Gemma, S.; Camodeca, C.; Coccone, S. S.; Joshi, B. P.; Bernetti, M.; Moretti, V.; Brogi, S.; de Marcos, M. C. B.; Savini, L.; Taramelli, D.; Basilico, N.; Parapini, S.; Rottmann, M.; Brun, R.; Lamponi, S.; Caccia, S.; Guiso, G.; Summers, R. L.; Martin, R. E.; Saponara, S.; Gorelli, B.; Novellino, E.; Campiani, G.; Butini, S. Optimization of 4-aminoquinoline/clotrimazole-based hybrid antimalarials: further structure−activity relationships, in vivo studies, and preliminary toxicity profiling. *J. Med. Chem.* **2012**, *55*, 6948−6967.
(29) Cornut, D.; Lemoine, H.; Kanishchev, O.; Okada, E.; Albrieux, F.; Beavogui, A. H.; Bienvenu, A.-L.; Picot, S.; Bouillon, J.-P.; Médebielle, M. Incorporation of a 3-(2,2,2-trifluoroethyl)-γ-hydroxy-γ-lactam motif in the side chain of 4-aminoquinolines. Syntheses and antimalarial activities. *J. Med. Chem.* **2013**, *56*, 73−83.
(30) Mott, B. T.; Cheng, K. C.-C.; Guha, R.; Kommer, V. P.; Williams, D. L.; Vermeire, J. J.; Cappello, M.; Maloney, D. J.; Rai, G.; Jadhav, A.; Simeonov, A.; Inglese, J.; Posnera, G. H.; Thomas, C. J. A furoxan−amodiaquine hybrid as a potential therapeutic for three parasitic diseases. *MedChemComm* **2012**, *3*, 1505−1511.
(31) Andayi, W. A.; Egan, T. J.; Gut, J.; Rosenthal, P. J.; Chibale, K. Synthesis, antiplasmodial activity, and β-hematin inhibition of hydroxypyridone−chloroquine hybrids. *ACS Med. Chem. Lett.* **2013**, *4*, 642−646.
(32) Manohar, S.; Rajesh, U. C.; Khan, S. I.; Tekwani, B. L.; Rawat, D. S. Novel 4-aminoquinolinepyrimidine based hybrids with improved in vitro and in vivo antimalarial activity. *ACS Med. Chem. Lett.* **2012**, *3*, 555−559.
(33) Pretorius, S. I.; Breytenbach, W. J.; Kock, C.; Smith, P. J.; N'Da, D. D. Synthesis, characterization and antimalarial activity of quinoline−pyrimidine hybrids. *Bioorg. Med. Chem.* **2012**, *13*, 3249−3261.
(34) Sharma, M.; Chaturvedi, V.; Manju, Y. K.; Bhatnagar, S.; Srivastava, K.; Puri, S. K.; Chauhan, P. M. Substituted quinolinyl chalcones and quinolinyl pyrimidines as a new class of anti-infective agents. *Eur. J. Med. Chem.* **2009**, *44*, 2081−2091.
(35) Singh, K.; Kaur, H.; Chibale, K.; Balzarini, J.; Little, S.; Bharatam, P. V. 2-Aminopyrimidine based 4-aminoquinoline anti-plasmodial agents. Synthesis, biological activity, structure−activity relationship and mode of action studies. *Eur. J. Med. Chem.* **2012**, *52*, 82−97.
(36) Singh, K.; Kaur, H.; Chibale, K.; Balzarini, J. Synthesis of 4-aminoquinoline−pyrimidine hybrids as potent antimalarials and their mode of action studies. *Eur. J. Med. Chem.* **2013**, *66*, 314−323.
(37) Natarajan, J. K.; Alumasa, J. N.; Yearick, K.; Ekoue-Kovi, K. A.; Casabianca, L. B.; de Dios, A. C.; Wolf, C.; Roepe, P. D. 4-*N*-, 4-*S*-, and 4-*O*-chloroquine analogues: influence of side chain length and quinolyl nitrogen pK_a on activity vs chloroquine resistant malaria. *J. Med. Chem.* **2008**, *51*, 3466−3479.
(38) Younis, Y.; Douelle, F.; Feng, T. -S.; González Cabrera, D.; Le Manach, C.; Nchinda, A. T.; Duffy, S.; White, K. L.; Shackleford, D. M.; Morizzi, J.; Mannila, J.; Katneni, K.; Bhamidipati, R.; Zabiulla, K. M.; Joseph, J. T.; Bashyam, S.; Waterson, D.; Witty, M. J.; Hardick, D.; Wittlin, S.; Avery, V.; Charman, S. A.; Chibale, K. 3,5-Diaryl-2-aminopyridines as a Novel Class of Orally Active Antimalarials Demonstrating Single Dose Cure in Mice and Clinical Candidate Potential. *J. Med. Chem.* **2012**, *55*, 3479−3487.
(39) Vennerstrom, J. L.; Ellis, W. Y.; Ager, A. L.; Anderaen, S. L.; Gerena, L.; Milhoust, W. K. *N*,*N*-Bis(7-chloroquinolin-4-yl) alkanediamines with potential against chloroquine-resistant malaria. *J. Med. Chem.* **1992**, *35*, 2129−2134.
(40) Egan, T. J.; Hunter, R.; Kaschula, C. H.; Marques, H. M.; Misplon, A.; Walden, J. Structure−function relationships in aminoquinolines: effect of amino and chloro groups on quinoline−hematin complex formation, inhibition of β-hematin formation, and anti-plasmodial activity. *J. Med. Chem.* **2000**, *43*, 283−291.
(41) Caron, G.; Reymond, F.; Carrupt, P. A.; Girault, H. H.; Testa, B. Combined molecular lipophilicity descriptors and their role in understanding intramolecular effects. *Pharm. Sci. Technol. Today* **1999**, *2*, 327−335.
(42) Lipinski, C. A.; Lombardo, F.; Dominy, B. W.; Feeney, P. J. Experimental and computational approaches to estimate solubility and permeability in drug discovery and development settings. *Adv. Drug Delivery Rev.* **2001**, *46*, 3−26.
(43) Avdeef, A. Physicochemical Profiling (Solubility, Permeability and Charge State). *Curr. Top. Med. Chem.* **2001**, *1*, 277−351.
(44) Warhurst, D. C.; Craig, J. C.; Adagu, I. S.; Meyer, D. J.; Lee, S. Y. The relationship of physicochemical properties and structure to the differential antiplasmodial activity of the cinchona alkaloids. *Malar. J.* **2003**, *2*, 26.
(45) Steyn, M.; N'Da, D. D.; Breytenbach, J. C.; Smith, P. J.; Meredith, S.; Breytenbach, W. J. Synthesis and antimalarial activity of ethylene glycol oligomeric ethers of artemisinin. *J. Pharm. Pharmacol.* **2011**, *63*, 278−286.
(46) Keyaerts, E.; Li, S.; Vijgen, L.; Rysman, E.; Verbeeck, J.; Ranst, M. V.; Maes, P. Antiviral activity of chloroquine against human coronavirus OC_{43} infection in newborn mice. *Antimicrob. Agents Chemother.* **2009**, *53*, 3416−3421.
(47) Ooi, E. E.; Chew, J. S. W.; Loh, J. P.; Chua, R. C. S. In vitro inhibition of human influenza A virus replication by chloroquine. *Virol. J.* **2006**, *3*, 39.
(48) Vincent, M. J.; Bergeron, E.; Benjannet, S.; Erickson, B. R.; Rollin, P. E.; Ksiazek, T. G.; Seidah, N. G.; Nichol, S. T. Chloroquine is a potent inhibitor of SARS coronavirus infection and spread. *Virol. J.* **2005**, *2*, 69.
(49) Kouroumalis, E. E. A.; Koskinas, J. Treatment of chronic active hepatitis B (CAH B) with chloroquine: a preliminary report. *Ann. Acad. Med.* **1986**, *15*, 149−152.
(50) Kono, M.; Tatsumi, K.; Imai, A. M.; Saito, K.; Kuriyama, T.; Shirasawa, H. Inhibition of human coronavirus 229E infection in human epithelial lung cells (L132) by chloroquine: involvement of p38 MAPK and ERK. *Antivir. Res.* **2008**, *77*, 150−152.
(51) Gans, P.; Sabatini, A.; Vacca, A. Investigation of equilibria in solution. Determination of equilibrium constants with the Hyperquad suite of programmes. *Talanta* **1996**, *43*, 1739−1753.
(52) Dascombe, M. J.; Drew, M. G. B.; Morris, H.; Wilairat, P.; Auparakkitanon, S.; Moule, W. A.; Alizadeh-Shekalgourabi, S.; Evans, P. G.; Lloyd, M.; Dyas, A. M.; Carr, P.; Ismail, F. M. D. Mapping antimalarial pharmacophores as a useful tool for the rapid discovery of drugs effective in vivo: design, construction, characterization, and pharmacology of metaquine. *J. Med. Chem.* **2005**, *48*, 5423−5436.
(53) Egan, T.; Ross, D.; Adams, P. Quinoline anti-malarial drugs inhibit spontaneous formation of beta-haematin (malaria pigment). *FEBS Lett.* **1994**, *352*, 54−57.
(54) Basilico, N.; Monti, D.; Olliaro, P.; Taramelli, D. Non-iron porphyrins inhibit L-haematin (malaria pigment) polymerization. *FEBS Lett.* **1997**, *409*, 297−299.

(55) Meshnick, S. R. Chloroquine as intercalator: a hypothesis revived. *Parasitol. Today* **1990**, *6*, 77−79.
(56) Wilson, W. D.; Jones, R. L. Intercalating drugs: DNA binding and molecular pharmacology. *Adv. Pharmacol. Chemother.* **1981**, *18*, 177−222.
(57) Cheng, J.; Zeidan, R.; Mishra, S.; Liu, A.; Pun, S. H.; Kulkarni, R. P.; Jensen, G. S.; Bellocq, N. C.; Davis, M. E. Structure−function correlation of chloroquine and analogues as trans gene expression enhancers in nonviral gene delivery. *J. Med. Chem.* **2006**, *49*, 6522−6531.
(58) Nikolis, N.; Methenitis, C.; Pneumatikakis, G. Studies on the interaction of altromycin B and palladium (II) metal complexes with Calf thymus DNA and nucleotides. *J. Inorg. Biochem.* **2003**, *95*, 177−193.
(59) Mudasir; Wahyuni, E. T.; Tjahjono, D. H.; Yoshioka, N.; Inoue, H. Inoue. Spectroscopic studies on the thermodynamic and thermal denaturation of the CT-DNA binding of methylene blue. *Spectrochim. Acta, Part A* **2010**, *77*, 528−534.
(60) Woynarowski, J. M.; Krugliak, M.; Ginsburg, H. Pharmacogenomic analyses of targeting the AT-rich malaria parasite genome with AT-specific alkylating drugs. *Mol. Biochem. Parasitol.* **2007**, *154*, 70−81.
(61) Trager, W.; Jensen, J. B. Human malaria parasite in continuous culture. *Science* **1976**, *193*, 673−675.
(62) Makler, M. T.; Ries, J. M.; Williams, J. A.; Bancroft, J. E.; Piper, R. C.; Gibbins, B. L.; Hinrichs, D. J. Parasite lactate dehydrogenase as an assay for *Plasmodium falciparum* drug sensitivity. *Am. J. Trop. Med. Hyg.* **1993**, *48*, 739−741.